49th AIAA Aerospace Sciences Meeting including the New Horizons Forum and Aerospace Exposition
4 - 7 January 2011, Orlando, Florida

AIAA 2011-577

Time-Accurate Flow Field and Rotor Speed Measurements of a Pulsed Detonation Driven Turbine

Kurt P. Rouser[1] and Paul I. King[2]
Air Force Institute of Technology, Wright-Patterson AFB, OH, 45433

Frederick R. Schauer[3] and Rolf Sondergaard[4]
U. S. Air Force Research Laboratory, Wright-Patterson AFB, OH, 45433

and

Larry P. Goss[5] and John L. Hoke[6]
Innovative Scientific Solutions, Inc., Dayton, OH, 45440

Time-accurate measurements of turbine inlet and exit flow fields and rotor speed are presented for a pulsed detonation driven radial turbine, using various instrumentation techniques: flush wall-mounted static pressure transducers, background oriented Schlieren, optical pyrometry, particle streak velocimetry, laser tachometers, and variable reluctance speed sensors. The primary motivation is to evaluate instrumentation methods with sampling frequencies greater than 10 kHz, acquiring data required for future unsteady turbine performance assessments. Time-resolved temperature, pressure, and velocity are required to calculate unsteady turbine efficiency, and time-resolved rotor speed is essential for describing turbine response to detonations. Previous experimental studies of pulsed detonations have not reported flow field temperatures, pressures, and velocities at high sampling frequencies. The operating environment in a pulsed detonation driven turbine is characterized by large, rapid excursions in temperature, pressure, and mass flow. Peak gas pressures, temperatures, and velocities are on the order of 60 atm, 3000 deg K, and 1000 m/s, respectively. Rotor speeds increase more than 15,000 RPM in less than 10 ms. The current work presents unsteady results for a Garrett T3-class automotive turbocharger driven by a pulsed detonation combustor. Evaluation of time-accurate flow field instrumentation techniques is made using measurements upstream and downstream of the pulsed detonation driven radial turbine. Additionally, a comparison of rotor speed instrumentation techniques is made with measurements of compressor blade passing frequencies.

Nomenclature

A	=	area
c_p	=	specific heat at constant pressure
I	=	moment of inertia
KE_{Rot}	=	rotational energy
$\dot{m}$	=	mass flow
P_t	=	pressure
T_t	=	temperature

---

[1] Graduate Student, Department of Aeronautics, AFIT/ENY, 2950 Hobson Way, Bldg 641, AIAA Associate Fellow.
[2] Professor, Department of Aeronautics, AFIT/ENY, 2950 Hobson Way, Bldg 641, AIAA Senior Member.
[3] Mechanical Engineer, Propulsion Directorate, AFRL/RZTC, 1790 Loop Rd, Bldg 490, AIAA Associate Fellow.
[4] Aerospace Engineer, Propulsion Directorate, AFRL/RZTT, 1950 Fifth St, Bldg 18, AIAA Associate Fellow.
[5] President, 2766 Indian Ripple Rd, AIAA Associate Fellow.
[6] Research Engineer, 2766 Indian Ripple Rd, AIAA Associate Fellow.

This material is declared a work of the U.S. Government and is not subject to copyright protection in the United States.

t = time
u = velocity
$\dot{W}$ = power
γ = ratio of specific heats
η = isentropic efficiency
ρ = density
τ = torque
ω = rotor speed

I. Introduction

DEVELOPMENT of hybrid pulsed detonation engine (PDE) and Brayton gas turbine engine (GTE) cycles exploits potential performance improvements from pressure-gain heat addition, including reduction in specific fuel consumption and increase in specific thrust and specific power. In 2002, Dyer and Kaemming[1] showed with a thermodynamic analysis that improvements in thermal efficiency result from lower entropy production associated with pressure gain combustion. In 2002, Hoke et al.[2] demonstrated concept feasibility using a detonation driven automotive turbocharger to self-aspirate a PDE. Experimental unsteady turbine efficiency; however, has yet to be reported for a full-admission pulsed detonation driven turbine.

Instrumentation methods and equations are well established to measure performance of conventional, steady Brayton GTEs; however, a hybrid PDE-GTE introduces unsteady effects that complicate performance evaluation. Conventional steady turbine performance is typically reported in terms of specific power and isentropic efficiency. In 2010, Rouser et al.[3] reported a 41% increase in time-average specific power and a 27% decrease in time-average brake specific fuel consumption with a pulsed detonation driven turbine compared to a steady deflagration driven turbine. For a thorough evaluation of unsteady detonation driven turbine performance, isentropic efficiency must also be known. In 2009, Suresh et al.[4] proposed several formulations for computing average isentropic efficiency for an unsteady turbine. They showed as much as a ten point difference could occur among various efficiency formulations.

This current work compares instrumentation techniques to acquire the flow field data of a PDC driven turbine. The objective is to evaluate various time-accurate measurements of turbine inlet and exit temperatures, pressures, and velocities needed to calculate turbine efficiency. Furthermore, this study compares instrumentation techniques to measure rotor speed, an essential parameter for characterizing the turbine response to detonations.

II. Background

Conventional steady isentropic turbine efficiency is based on inlet and exit gas temperatures and pressures and constant specific heat, as shown in Eq. (1). Operating conditions of a full-admission PDC driven turbine are characterized by rapid excursions in pressure and temperature with peak detonation pressures on the order of 60 atm, flame temperatures of about 3,000 deg K, and peak detonation exhaust velocities near 1,000 m/s. Furthermore, the unsteady nature of the flow complicates the conventional steady control volume turbine efficiency formulation because of the need for a ratio of flow field properties at the same instant in time. High frequency events in the pulsed detonation cycle, such as the von Neumann spike, size the time scale and determine the minimum sampling rate. In this study, the detonation firing sequence has a 22 ms duration and consists of five distinct events. Therefore, the shortest event occurs in about four milliseconds. To satisfy Nyquist criteria, the minimum sampling frequency is 500 Hz. For better time resolution of detonation events, this study used a minimum sampling frequency of 10 kHz. The magnitude of turbine efficiency is expected to vary significantly over the PDC cycle, as the turbine does not necessarily remain choked.

$$\eta_{turbine} = \frac{1-\left(\dfrac{T_{t,exit}}{T_{t,inlet}}\right)}{1-\left(\dfrac{P_{t,exit}}{P_{t,inlet}}\right)^{\frac{\gamma-1}{\gamma}}} \tag{1}$$

In 2007, Glaser et al.[5] reported unsteady turbine power and efficiency for a dual-stream axial turbine with an array of PDCs, in which detonation exhaust mixed with steady bypass air before entering the turbine. An eight-to-one ratio of steady bypass air to unsteady detonation exhaust produced a suitably steady environment for conventional instrumentation to measure moderate pressures and temperatures; however, no significant performance improvements over steady deflagration driven turbine operation were observed. Mixed flow turbine performance may have been adversely affected by secondary flow effects[6].

Suresh et al.[4] compared two formulations of average turbine efficiency for unsteady flows. Both formulations integrated total temperature, T_t, total pressure, P_t, density, ρ, and velocity, u, at inlet and exit planes over pulsed detonation cycle time, T. The first formulation (Eq. 2) was based on the assumption that the ideal turbine expands the flow instantaneously.

$$\bar{\eta}_{turbine} = \frac{\int_T \left(\int_{A_{inlet}} (\rho u T_t) dA \right) dt - \int_T \left(\int_{A_{exit}} (\rho u T_t) dA \right) dt}{\int_T \left(\int_{A_{inlet}} (\rho u T_t) dA \right) dt - \int_T \left(\int_{A_{inlet}} \frac{\rho u T_t}{P_t^{\frac{\gamma-1}{\gamma}}} dA \cdot \frac{1}{|A_{exit}|} \int_{A_{exit}} P_t^{\frac{\gamma-1}{\gamma}} dA \right) dt} \tag{2}$$

The second formulation (Eq. 3) was based on work averaging, which defines average unsteady flow in a manner that preserves work inflow or outflow to/from an isentropic turbine. The resulting expression was based on time-averaged, mass-averaged total temperatures and work-averaged total pressures.

$$\bar{\eta}_{turbine} = \frac{T_{t,inlet}^{avg} - T_{t,exit}^{avg}}{T_{t,inlet}^{avg} \left(1 - \left(\frac{P_{t,exit}^{work-avg}}{P_{t,inlet}^{work-avg}} \right)^{\frac{\gamma-1}{\gamma}} \right)} \tag{3}$$

Alternative unsteady turbine efficiency formulations are possible, requiring flow field properties of pressure, temperature, and velocity. The difference between formulations is in the manner in which transients of the ideal unsteady turbine are characterized.

Understanding turbine response guides turbine design and integration into a PDE-GTE hybrid system. Insight into transmission and storage of power is possible using formulations of torque, power, and change in rotational energy, which are based on rotor speed.

$$\tau(t) = I \frac{d\omega(t)}{dt} \tag{4}$$

$$\dot{W}(t) = \tau(t) \cdot \omega(t) \tag{5}$$

$$\Delta KE_{rot} = \tfrac{1}{2} \left(I\omega_{\max}^2 - I\omega_{\min}^2 \right) \tag{6}$$

Sampling frequencies of rotor speed must sufficiently capture dynamics associated with pulsed detonations and with blade passing frequencies. Blade passing frequencies are a function of blade count and rotor speed. The nine-blade, radial turbine used in this study is part of a Garrett GT28 automotive turbocharger, pictured in Fig. 1. The turbine wastegate is capped so that all combustor exhaust passes through the turbine. The GT28 is also equipped with a radial compressor having six primary impeller blades and six splitter blades. The GT28 compressor map is shown in Fig. 2 with lines of corrected rotor speed. The center of the map includes rotor speeds around 115,000

RPM, which relates to compressor blade passing frequencies of 23 kHz. To satisfy Nyquist frequency criteria, rotor speed sampling frequencies for this research must exceed 46 kHz.

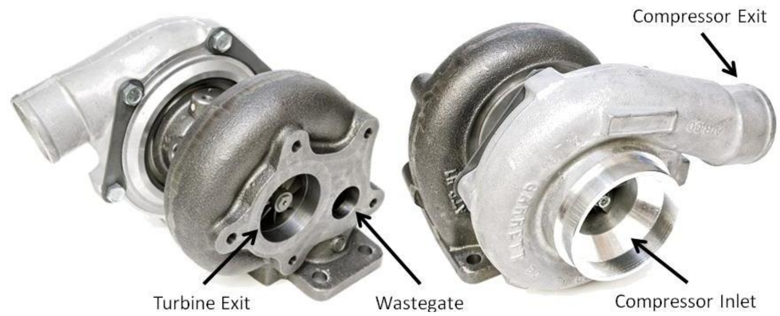

Fig. 1. Garrett GT28 automotive turbocharger (used with permission).

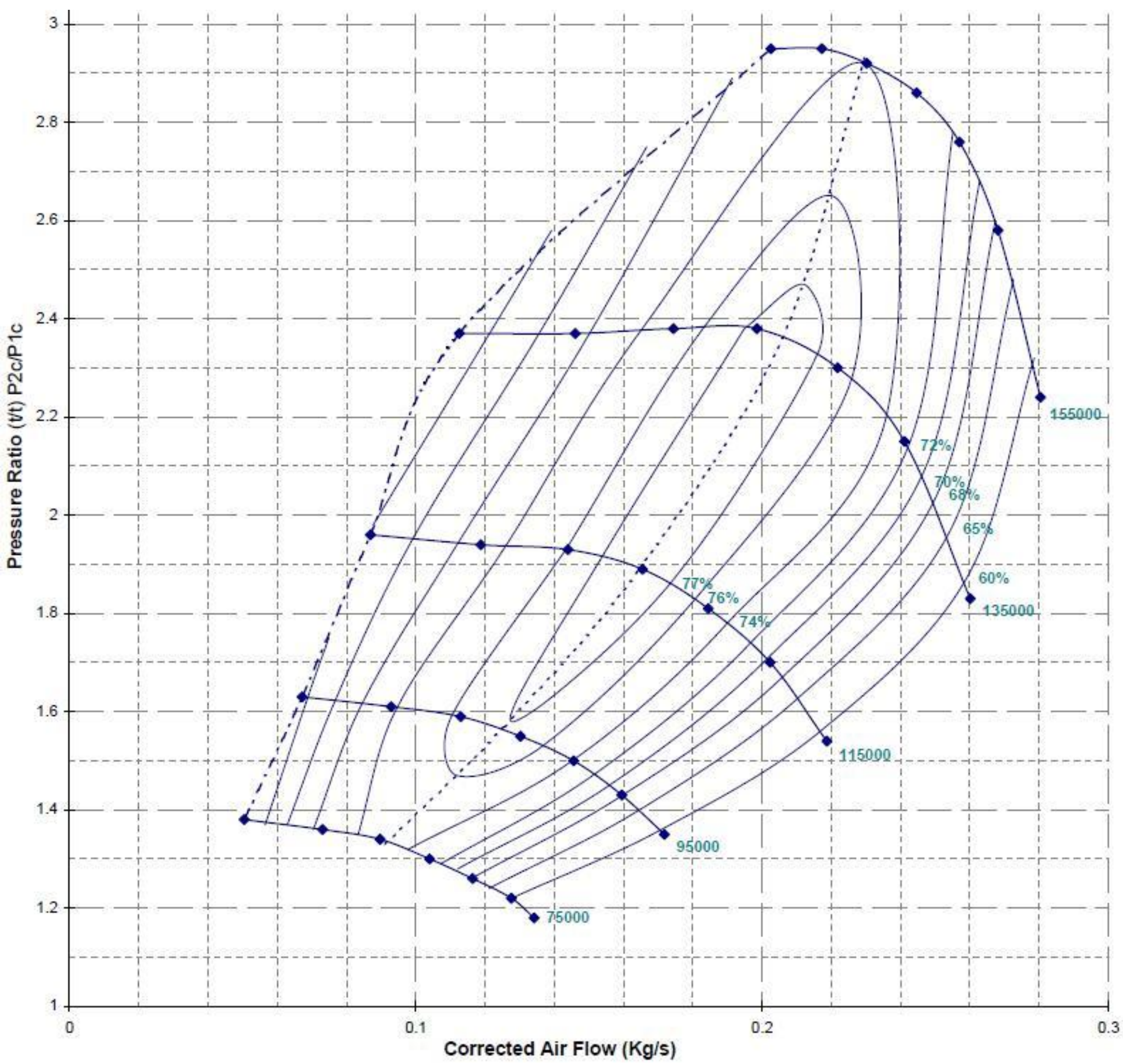

Fig. 2. Garrett GT28 compressor operating map (used with permission).

The pulsed detonation cycle is characterized by three major phases: fill, fire and purge, as depicted in Fig. 3. For this study, the duration of each phase was about equal and depended on the operating frequency. During the fill phase, fuel/air mixture enters the chamber at near ambient temperature and about twice the ambient pressure. The fill velocity is subsonic and depends primarily on chamber geometry and mass flow rate, which is related to the desired volumetric fill fraction and operating frequency. Excursions during the fill phase relate to fill velocity, pressure waves from opening and closing valves, and heat transfer through the chamber walls. The fire phase consists of four parts: ignition, deflagration to detonation transition (DDT), detonation, and blowdown. Figure 4 shows a notional timeline during the fire phase, with an initial delay for optimal ignition timing. The detonation wave speed at the turbine inlet is on the order of 1,000 m/s; however, the inlet flow field is relatively stationary during the fire phase until detonation wave arrival. Excursions during the fire phase relate to the characteristics of each of the constituent events. Excursions during the purge phase are very similar to those in the fill phase, though the purge fraction may be different than the fill fraction. Thus, flow field properties entering the turbine are very unsteady, with high peak pressures, temperatures, and velocities, as well as rapid transients between the events that comprise the pulsed detonation cycle. The largest, most rapid excursions occur during fire phase.

Fig. 3. Pulse detonation combustor phases with timing for 15 Hz operating frequency.

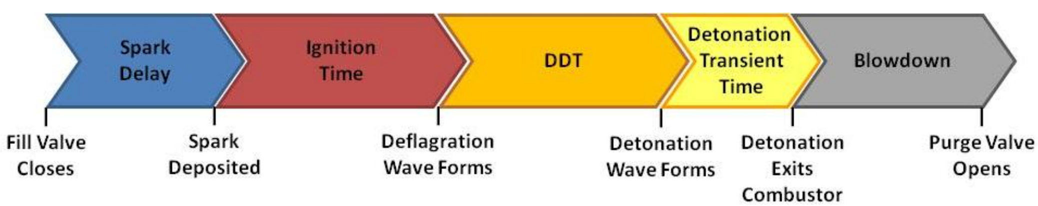

Fig. 4. Notional timeline of events in fire phase.

III. Experimental Arrangement and Methodology

Experiments were carried out in the Air Force Research Laboratory (AFRL) Pulse Detonation Research Facility, using configurations similar to previous work[2-3]. The facility supplied compressed air to the main fill and purge manifolds as seen in Fig. 5. Fuel was mixed at the entrance to the main manifold. Fill distribution and ignition took place using an automotive engine head and cam to operate intake and exhaust valves for desired operating frequencies. The intake valves were used for the main fill fuel-air mixture, and the exhaust valves were used to inject purge air. During the fire phase, intake and exhaust valves were closed.

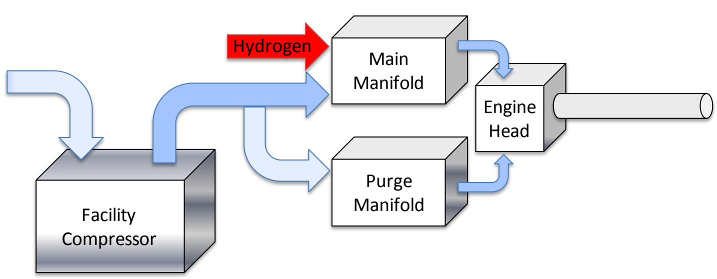

Fig. 5. AFRL Pulse Detonation Research Facility engine test block diagram.

A. Pulsed Detonation Combustor and Turbocharger Arrangement

The PDC in this experiment was a two-inch diameter steel pipe that is three feet (1.22 m) in length. An internal spiral 18 inches (45.7 cm) in length assisted DDT. Two ion probes were installed 18 inches (45.7 cm) and 24 inches (61 cm) downstream of the spiral to verify Chapman-Jouguet velocities. The probes short-out when the flame front arrives, and velocity is determined from the transit time between probes. PDC start-up operation was attained by first setting desired air flow and operating frequency. Then, start-up spark ignition occurred as fuel was added until a desired equivalence ratio was achieved, by which time the detonation cycle was established. The turbine inlet of the turbocharger was coupled to the PDC exit as shown in Fig. 6. All of the mass flow from the PDC entered the turbocharger. Before the first detonation, the turbocharger turbine was driven by the fill and purge phases associated with the start-up sequence.

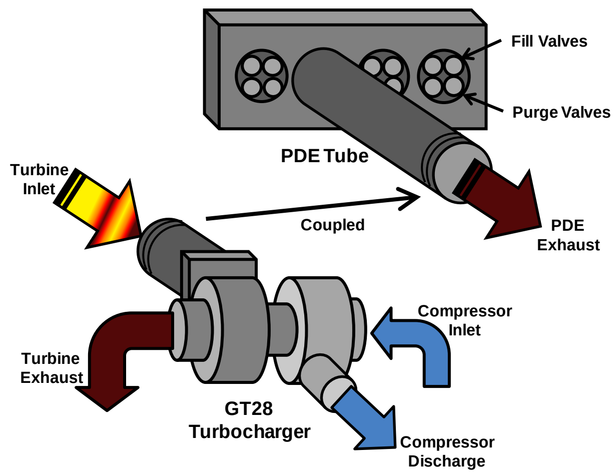

Fig. 6. PDC and turbocharger test rig.

B. Standard Pulsed Detonation Combustor and Turbocharger Instrumentation

The compressor side of the turbocharger received ambient air through a mass air flow (MAF) sensor located 24 inches (61 cm) upstream of the compressor inlet. A wall-mounted 50 psi (344 kPa) static pressure transducer and J-type thermocouple were located 16 inches (40.6 cm) and 20 inches (50.8 cm) upstream of the compressor inlet, respectively, as seen in Fig. 7. The compressor discharge was instrumented with a wall-mounted 50 psi (344 kPa) static pressure transducer located 46 inches (1.17 m) downstream of the compressor exit along a two inch (52 mm) diameter pipe, as shown in Fig. 7. A J-type thermocouple was located six inches (15.2 cm) downstream of the pressure transducer. A ball valve, located 24 inches (609 mm) downstream of the thermocouple, was used to back-pressure the compressor. The ball valve was set so that the compressor operated toward the center of its operating map. Thus, the compressor served as a dynamometer to measure compressor power.

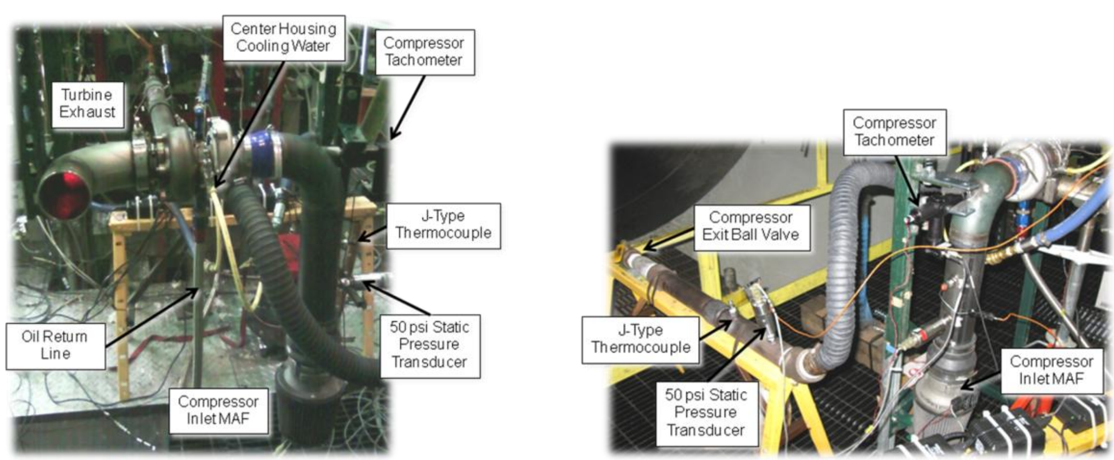

Fig. 7. Turbocharger instrumentation and control valve.

C. Rotor Speed Measurement Techniques

Two different rotor speed instrumentation packages were used during testing. A Garrett speed sensor (part number #781328-0002) was positioned in the compressor housing, as shown in Fig. 8, to detect blades arrival. The sensor emits a magnetic field that is interrupted by passing blades. Rotor speed is determined from the blade passing frequency. The input frequency is one pulse per blade. The internal sensor electronics divide the input signal by eight, so that the output frequency is a square-wave signal at $1/8^{th}$ the actual blade passing frequency. The output frequency is multiplied by eight during post-processing to obtain in the input frequency. The turbocharger compressor has 12 blades with a blade passing frequency of about 23 kHz.

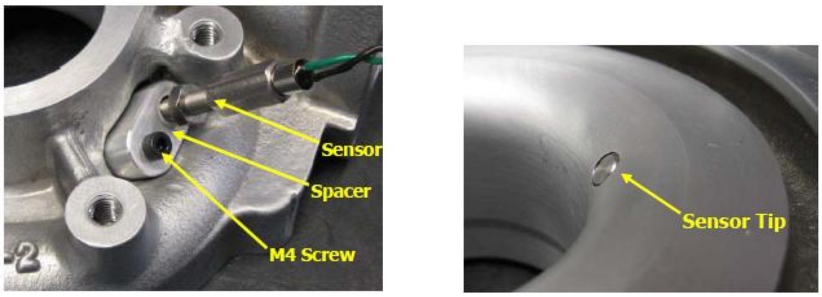

Fig. 8 Garrett speed sensor (used with permission)

The second rotor speed measurement was made with laser tachometers positioned at the compressor inlet and turbine exhaust, as shown in Fig. 9. Each tachometer was comprised of a 4 mW, 670 nm diode laser with a collimating lens that focused a beam on compressor blade leading edges and turbine blade trailing edges, as shown in Fig. 9. The return beam deflected off an internal mirror toward a photodiode with a switchable-gain, amplified silicon detector. Blade arrival was indicated by a peak signal from the photodiode. As with the Garrett sensor, rotor speed was determined by the difference in blade arrival times. The photodiode output frequency matched the blade passing frequency. A time history of the compressor blade passing frequency is shown in Fig. 10 for a 10 Hz PDC driven turbine with cold flow (no ignition). The compressor tachometer does not detect the six secondary splitter blade leading edges, which are concealed by the six primary blades. In hot flow (with detonations) the turbine laser tachometer photodiode was saturated by the flame illumination, preventing the detection of blade trailing edges. Though this effect was limited to a brief period, the timing coincides with the rapid acceleration in rotor speed. Therefore, the compressor tachometer results are used for rotor speed in this study, not the turbine tachometer.

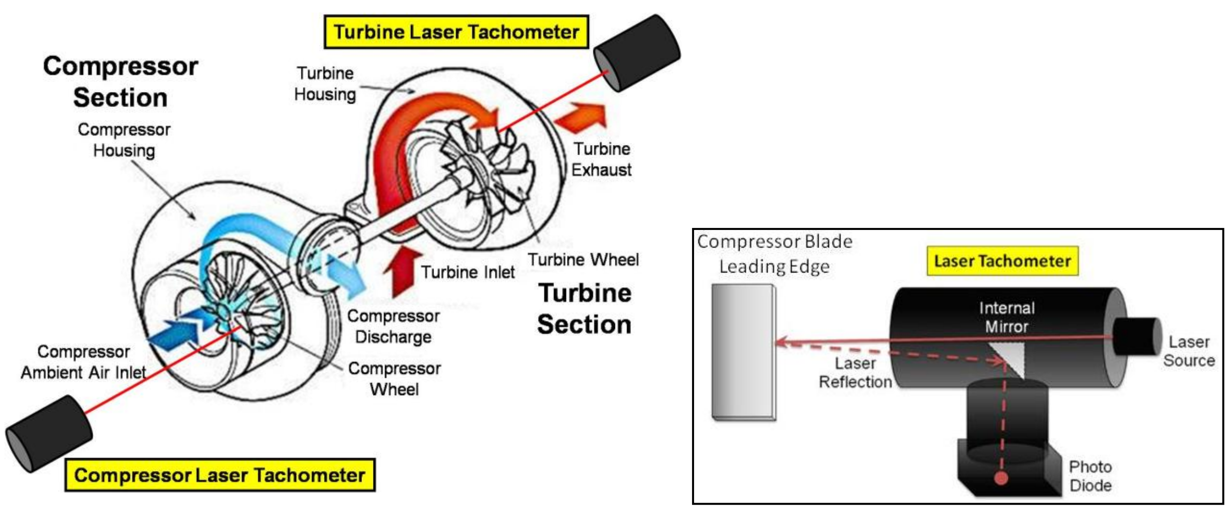

Fig. 9. Turbocharger tachometer schematic (used with permission).

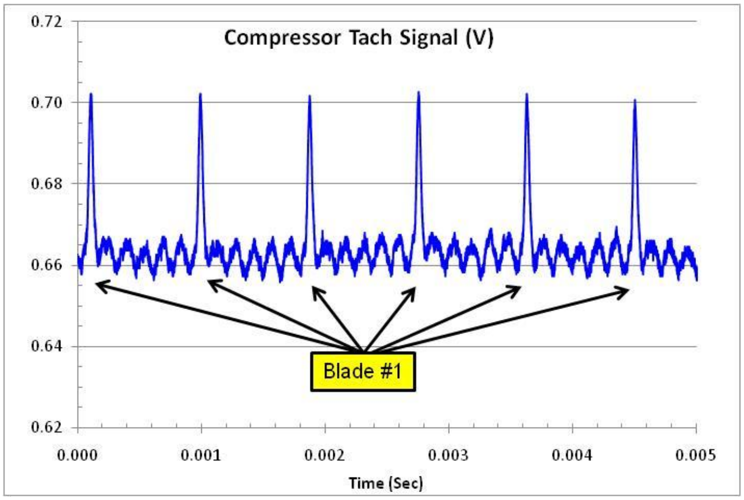

Fig. 10. Compressor tachometer signal with cold flow at 10 Hz operating frequency.

D. Turbine Inlet and Exit Flow Field Measurement Techniques

Table 1 includes a summary of the various flow field instrumentation techniques employed in this research. A combination of these techniques will be used to collect the necessary flow field data to calculate unsteady turbine efficiency. Static pressure transducers were flush mounted on the inlet and exhaust tube walls. The inlet transducer was located 1 inch (25.4 mm) upstream of the turbocharger turbine inlet flange. The exit transducer was located six inches (152 mm) downstream of the turbine.

Table 1. Time-accurate turbine inlet and exit flow measurements

Technique	T_in	T_exit	P_in	P_exit	u_in	u_exit
Wall-Mounted Static Pressure Transducer			X	X		
Two Color Band Optical Pyrometry	X	X				
Particle Streak Velocimetry (PSV)					X	
Background Oriented Schlieren (BOS)				X*		X
*Note: The BOS technique provides density, which will ultimately produce pressure data when combined with temperature data from optical pyrometry						

1. Two Color Band Pyrometry.

For optical pyrometry temperature and PSV velocity measurements, a square pipe section with a 2 in x 2in (51 mm x 51 mm) cross section, one foot (305 mm) in length, and two side-mounted quartz windows was mounted upstream of the turbocharger turbine, as shown in Fig. 11. A square pipe section with a 2 in x 2in (51 mm x 51 mm) cross section, three foot (915 mm) in length, and with two side-mounted plexiglass windows was mounted downstream of the turbine, coupled to the turbine exhaust elbow with a pipe reducer. To demonstrate the capability of a high speed color camera to capture temperature fields in combustion systems, a PCO Dimax high-speed color camera was used. Measurements with a tungsten lamp and spectrometer allowed the spectral responsivity of the red, green and blue channels of this camera to be measured (see Fig. 12 left graph). Substituting the spectral responses and integrating them with a blackbody function over the appropriate wavelengths allows the ratio to be determined as a function of temperature (see Fig. 12 right graph).

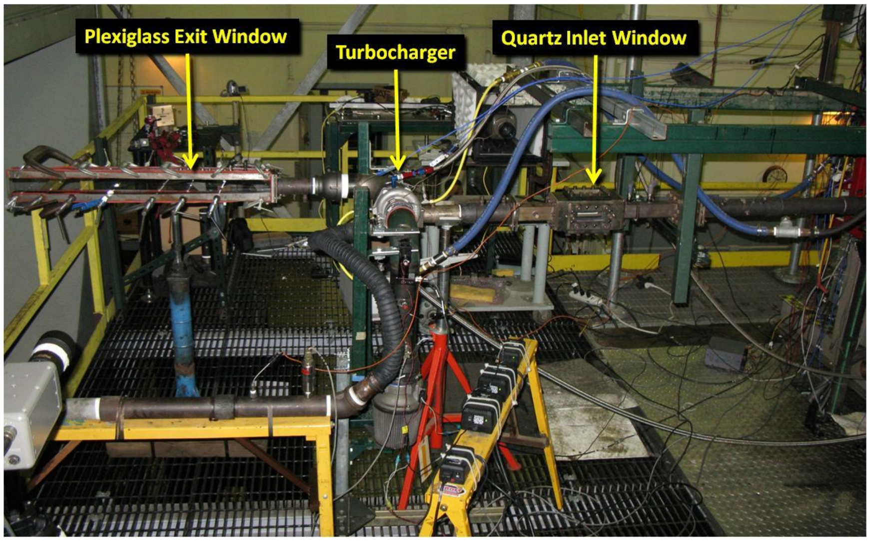

Fig. 11. Turbine inlet and exit window arrangements.

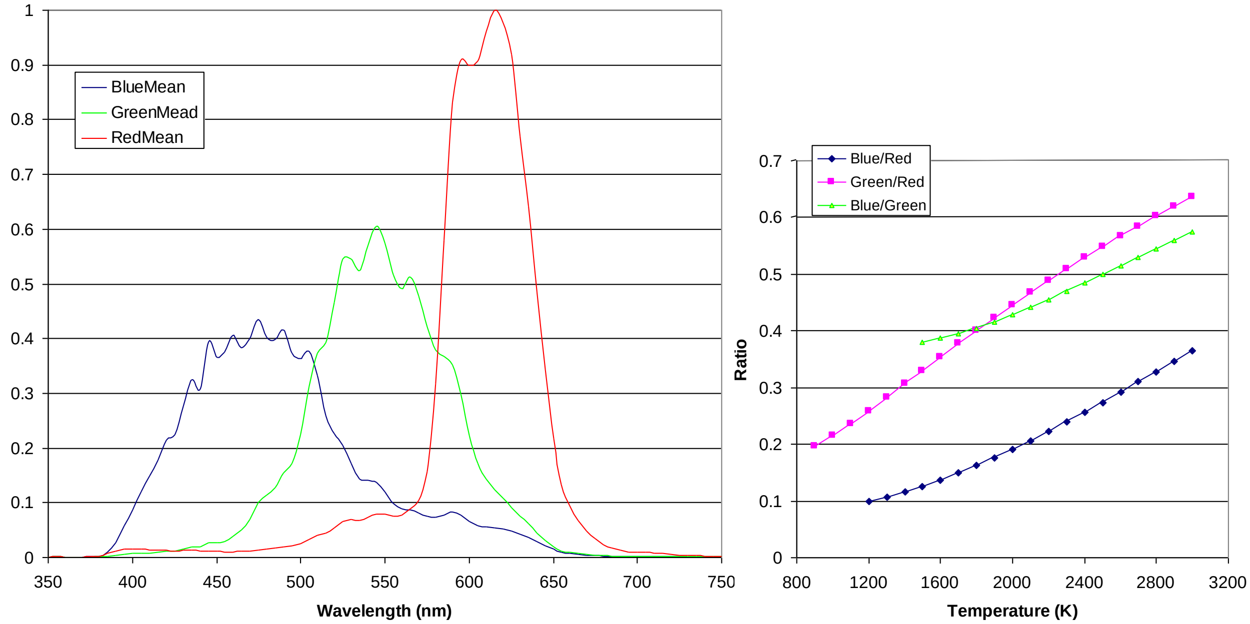

Fig. 12. Left graph: PCO Dimax camera relative responsivity for the blue, green and red channels as a function of wavelength. Right graph: ratio of the various color channels for a PCO Dimax camera as a function of temperature for a black or gray body emitter

Soot is only formed in the fuel rich areas of flames and may not be present in a combustion region of interest. Therefore, silicon carbide (SiC) seed particles (1-2 µm in size) have been used for seeding combustion flow fields. SiC filaments have been used for thermometry for many years. The technique termed Thin Filament Pyrometry[7] (TFP) has been used in a variety of laboratory flame systems. Graybody emission from the filament is recorded and used to determine flame temperature. Because the filament is small, the temporal response of the filament to temperature changes is high (>1,000 Hz). The technique is somewhat limited, however, by the fragility of the small 10 µm filaments. To overcome this limitation, SiC particles are used to seed combustion flow, rather than filaments. Figure 14 shows the temperature field of a SiC-seeded flow in a pulsed detonation engine. The SiC particles, 2400 grit size, were injected into the PDC fuel line with a standard dry cyclone seeder. The PCO Dimax camera was operating with a 1.5 µs exposure and 87 µs inter-frame time to achieve a frame rate of 11,484 frames/s.

Temperatures shown in Fig. 13 were recorded along the centerline. Pyrometry data could only be collected when particles were at high enough temperatures to produce sufficient emission. Thus, pyrometry temperature data was not available during fill and purge phases.

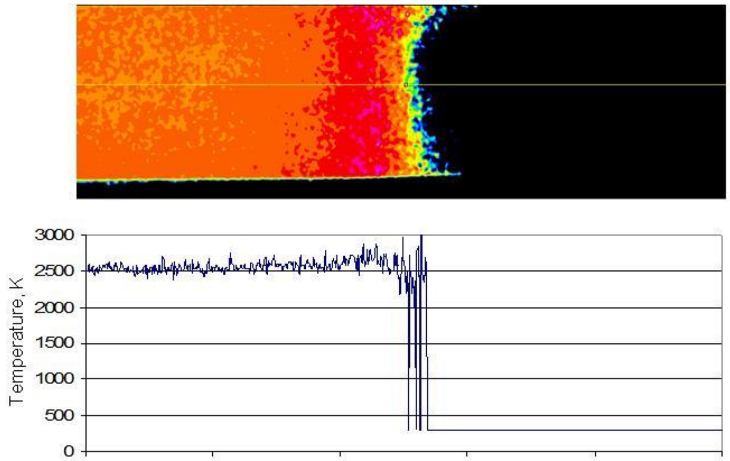

Fig. 13. Single frame of pyrometry results for a detonation flame front travelling from left to right in a detonation tube, in which black represents unburned fuel-air. Lower graph is temperature profile along centerline.

2. Particle Streak Velocimetry.

PSV measurements were taken through the quartz window at the turbine inlet to determine the velocity of the PDC gases after the detonation front. When using ethylene fuel, a significant amount of soot was formed in exhaust gases at stoichiometric conditions. By increasing exposure time of the PCO Dimax high-speed camera from 1 to 10 μs, time history of the soot particle streaks were traced from frame to frame. The turbine inlet velocity field was determined by dividing the length of a particle streaks by the exposure time, as shown in Fig. 14. To increase the contrast between the soot streaks and the surrounding gas emission, an edge enhancing convolution was applied to the image before analysis. Ultimately, PSV measurements will be obtained with SiC seed particles.

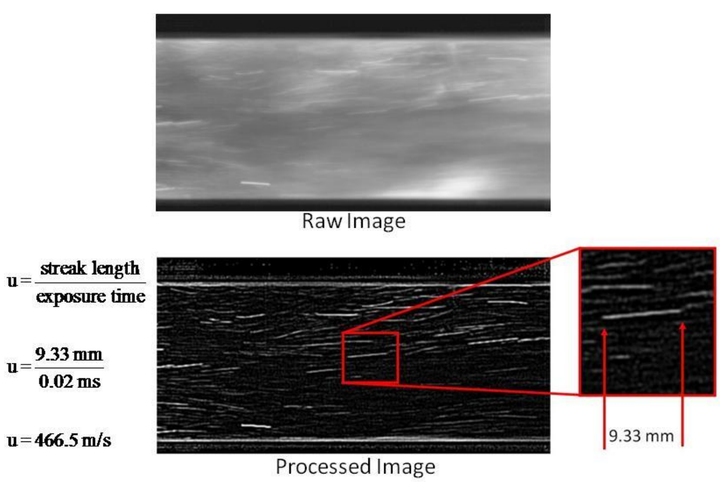

Fig. 14. Particle streak velocimetry image during blowdown at the turbine inlet.

3. Background Oriented Schlieren.

BOS is an optical measurement technique that has the ability to visualize density gradients. BOS was proposed by Meier in 1999[8] and can be described as a simple Schlieren technique based on image displacements of a background caused by density gradients in the optical path. A major advantage of the technique is that it requires only a digital camera of sufficient resolution to allow background displacements to be accurately captured. The background displacements are typically determined using particle image velocimetry (PIV) based correlation methods which are well established. Early studies demonstrated several possible applications of BOS for determining density fields of helicopter-generated vortices[9] and supersonic jets[10]. Recent work has demonstrated quantitative visualization of density flow in an axisymmetric cone-cylinder in a Mach 2,0 flow. Meier[11] (2004) successfully validated the BOS technique by comparing the cone cylinder results with data from cone tables and isentropic solutions. The kilo-hertz capability of the BOS technique was demonstrated in 2009 when it was successfully used to capture transient igniter temperatures at rates in excess of 24,000 frames per second[12].

The BOS technique was chosen for this study because of its ability to function with high speed cameras, which allow density field images of pulsed detonation exhaust to be captured at a very high rate. To achieve these high rates, a Phantom v7 was utilized in conjunction with an over-driven pulsed LED array[13]. High framing rates required that the BOS background be setup in a transmission mode with the LED array arranged as a back light. This ensured that the maximum amount of light was available to the Phantom camera, which helped to minimize the pulse width of the LED array (~1μs) and allowed the use of a large f# (22) needed for increased sensitivity and measurement resolution.

The experimental arrangement used to capture the BOS data is shown in Fig. 15. The output of the pulsed LED array was directed through a series of scattering glass plates that formed the random background needed for the BOS experiment. The background image from the scattering plate was recorded with a high speed cine Phantom v7 camera with a 500 ns exposure and 122 μs inter-frame time. Transient density gradients caused by the PDC-turbine exhaust pulse distorted the background image and were recorded by the Phantom camera. The displacement of the background due to the density field was determined by conducting a correlation analysis between the non-disturbed image (no flow) and the gradient disturbed images (flow). This is an established approach used in PIV analysis where particle movement between successive images is correlated to yield the velocity field. If the temperature field or pressure field is know from an independent measurement, then either the transient-temperature or transient-pressure can be determined from the density field.

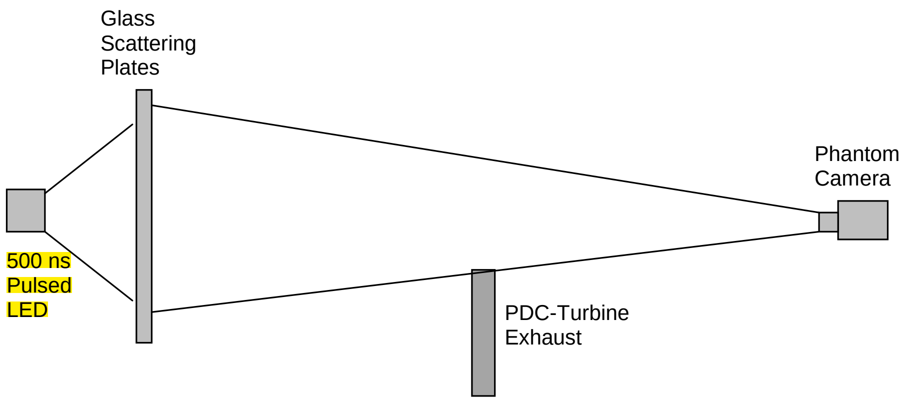

Fig. 15. Background oriented Schlieren arrangement utilized for high-speed visualization, density and velocity measurements at the PDC driven turbine exit.

Figure 16 shows the BOS displacement vector magnitudes in the flow field of the pulsed detonation driven turbine exit. Not only was the BOS technique used to determine density, it was also used to measure the velocity of the density structures. To accomplish this task, the displacement magnitude images were correlated (using PIV analysis software) to yield the gradient density velocity.

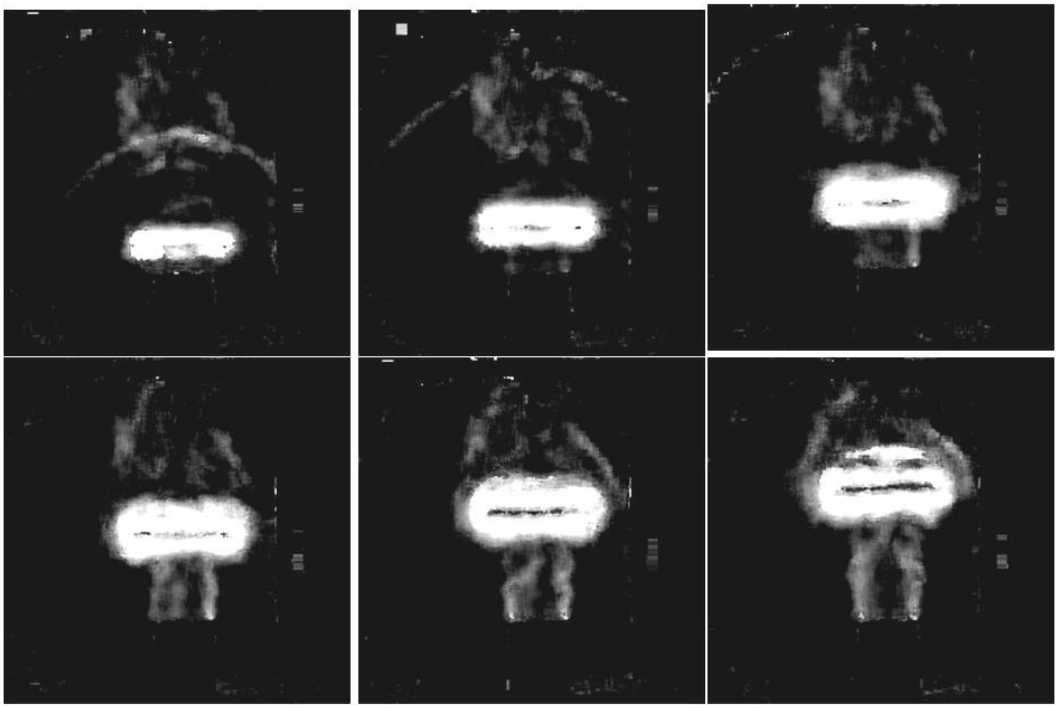

Fig. 16. Six frames of background oriented Schlieren vector magnitude plots for a pulsed detonation turbine exhaust flow field. Flow in each image is from bottom to top, and the sequence proceeds from left to right.

IV. Results

Figure 17 shows a sample trace of rotor speed history from the compressor laser tachometer for a 10 Hz PDC with a fill fraction of 1.0 and a purge fraction of 0.3. Scatter in rotor speed data is attributed to vibration induced by the PDC. A simple arithmetic average of rotor speed was 66,716 RPM with the major peak corresponding to the effects of fire phase. The spark signal trace included in Fig. 17 indicates the start of the fire phase at about 30 ms, and the signal peak from the turbine laser tachometer photodiode indicates the detonation wave exits the turbine at about 40 ms. The rotor speed rises just after the detonation wave exits the turbine, and peak rotor speed occurs about 10 ms later.

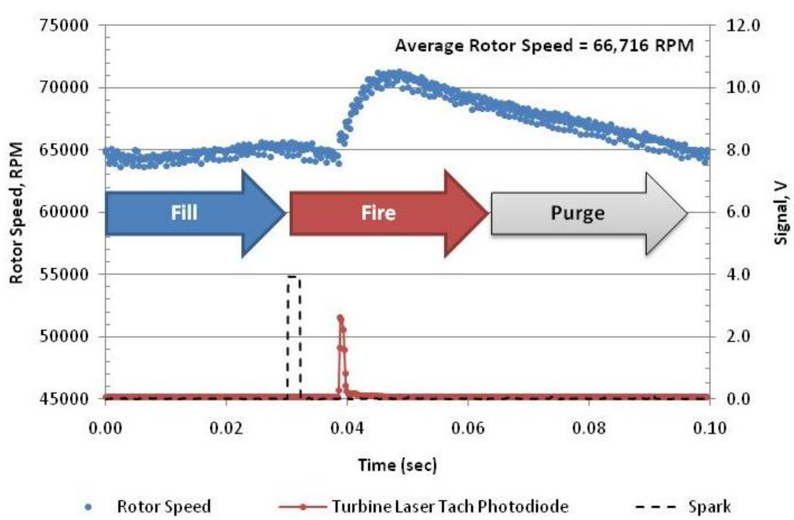

Fig. 17. Rotor speed history using the compressor laser tachometer for 10 Hz PDC driven turbine (fill fraction = 1.0, purge fraction = 0.3).

Figure 18 shows compressor rotor speed history from the Garrett speed sensor over three detonation cycles for a 15 Hz PDC with a fill fraction of 1.0 and a purge fraction of 0.5. The data is less scattered than with the laser tachometer, due to the 1/8th frequency filter; however, there is also less resolution around the time that the detonation arrives at the turbine (about 0.06 ms). There is good periodicity between detonation events, and the rotor speed climbs about 15,000 RPM. Peak rotor speed occurs in less than 10 milliseconds, as was observed with the laser tachometer.

Both compressor rotor speed measurement techniques capture the magnitudes and transients associated with the turbine response to detonations. The sharp acceleration that occurs with the detonation arrival indicates a large shaft torque. Whereas the Garrett sensor produces a rotor speed trace with less scatter, it is also less resolved around the detonation arrival time at the turbine.

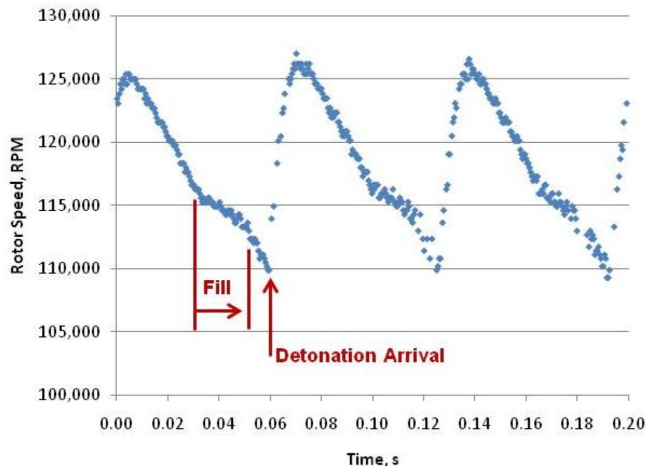

Fig. 18. Compressor rotor speed history using a Garrett speed sensor for 15 Hz PDC driven turbine (fill fraction = 1.0, purge fraction = 0.5).

Figure 19 shows time history of static pressure at the turbine inlet and exit during the fire phase for a 15 Hz PDC with a fill fraction of 1.0 and a purge fraction of 0.5. Peak inlet pressure is nearly 150 psia, which is less than the expected 60 atm magnitude of the von Neumann pressure spike associated with a detonation wave. This single point measurement technique to obtain pressures may not necessarily be representative of the average 2-D pressure field.

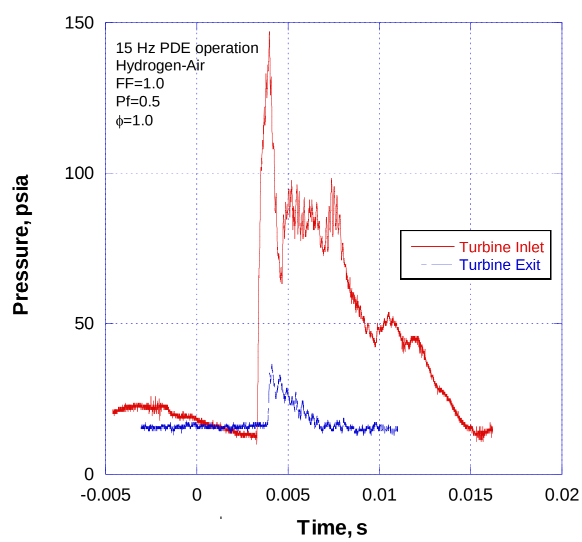

Fig. 19. Turbine inlet and exit wall static pressures for a 15 Hz PDC driven turbine (fill fraction = 1.0, purge fraction = 0.5).

Figure 20 shows turbine inlet and exit flow field velocity results from PSV and BOS 1-D point measurements, respectively, for a 15 Hz PDC with a fill fraction of 1.0 and a purge fraction of 0.5. The velocity is shown over the blowdown portion of the PDC fire phase (see Fig. 3 and Fig. 4). The initial inlet gas velocity appears high, possibly due to an expected Taylor wave following the detonation front. The large inlet velocity fluctuations are damped by the turbine, such that the exit velocity is more linear. The turbine inlet velocity excursions include momentary reverse flow.

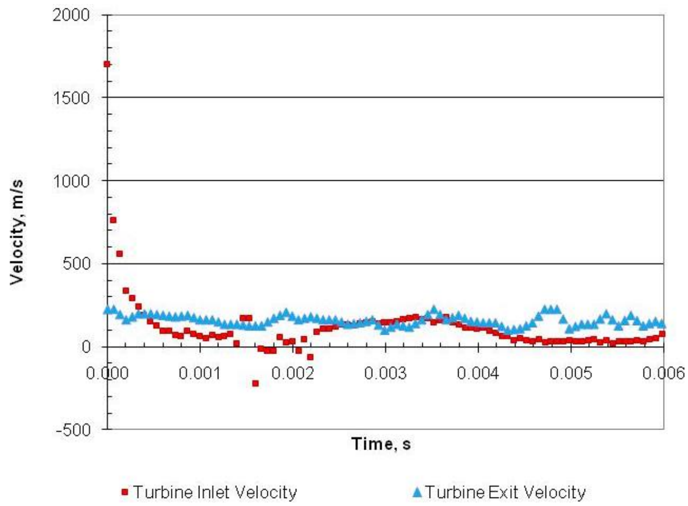

Fig. 20. Turbine inlet and exit velocities from PSV measurements for a 15 Hz PDC driven turbine (fill fraction = 1.0, purge fraction = 0.5).

Figure 21 shows pyrometry turbine inlet and exit static temperatures for a blowdown event at 15 Hz PDC operation with a fill fraction of 1.0 and a purge fraction of 0.5. The temperature data was taken at a single centerline point. The initial inlet gas temperature exceeds the adiabatic flame temperature for hydrogen because of the elevated combustion pressure. The exit temperature is nearly constant, but drops quickly at the end of the blowdown. The difference between the inlet and exit temperatures indicates a drop in enthalpy across the turbine.

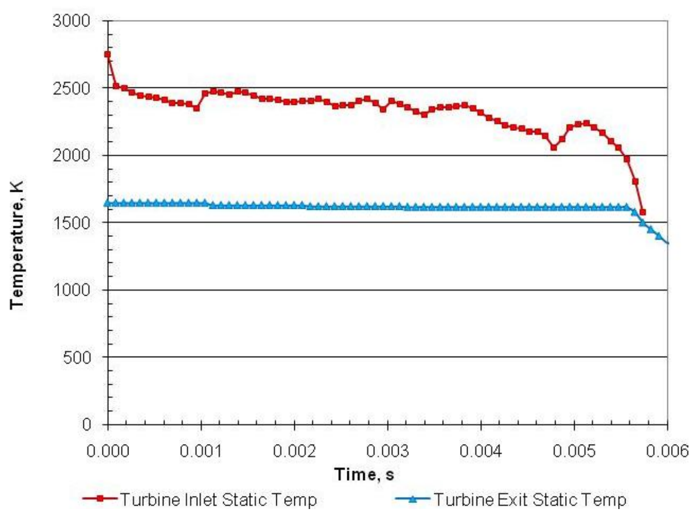

Fig. 21. Turbine inlet and exit static temperatures from optical pyrometry measurements for a 15 Hz PDC driven turbine (fill fraction = 1.0, purge fraction = 0.5).

V. Conclusions and Recommendations

Whereas previous experimental work[2,3] demonstrated the capability of a PDC to drive a turbine, and numerical studies have compared formulations of unsteady turbine efficiency[4], this current work evaluated various instrumentation techniques to acquire the flow field data of a PDC driven turbine, which are necessary to calculate turbine efficiency. Furthermore, this study compared instrumentation techniques to measure rotor speed, which is essential to characterizing the turbine response to detonations. Static pressure transducers adequately captured 1-D magnitudes of gas pressures and pressure ratio across the turbine. Use of SiC particles made it possible to use a combination of optical pyrometry and particle streak velocimetry to obtain temperature and velocity. The results included expected magnitudes and flow field transients. The background oriented Schlieren (BOS) technique was able to provide velocity and density flow field. Turbine exit velocities obtained from the BOS measurements did not fluctuate as much as the inlet velocities obtained from PSV. The BOS density results showed good potential for obtaining 2-D flow field pressures by combining results from optical pyrometry. Rotor speed from compressor blade passing frequencies obtained with a laser tachometer and a Garrett speed sensor were also similar. Laser tachometer results had better resolution of the rotor acceleration; however, there was some scatter in the laser speed data.

Future work will employ instrumentation techniques from this study to evaluate unsteady turbine efficiency. Temperature, pressure, and velocities will be obtained to compare unsteady turbine performance driven by pulsed detonations to the manufacturer's published steady turbine efficiency. Furthermore, different formulations of turbine efficiency should be evaluated with experimental data, using a turbine with known steady turbine efficiency. A thorough performance evaluation of a turbine driven by pulsed detonations can be made by assessing specific power and isentropic turbine efficiency. Future work is also recommended to evaluate torque, power, and rotational energy using rotor speed instrumentation from this study.

Acknowledgments

The authors thank the Pulse Detonation Research Facility team for frequent support that made this research possible, especially Andrew Naples, Curtis Rice, David Burris, and Christopher Stevens. Additionally, Corey Goss supported the laser and optical instrumentation work. Appreciation is also expressed to Dr. Robert Hancock (AFRL/RZT) and Dr. Joseph Zelina (AFRL/RZTC) for their technical leadership. Funding was provided by the Air Force Research Laboratory, Propulsion Directorate and AFOSR.

References

[1]Dyer, R.S., and Kaemming, T.A., "The Thermodynamic Basis of Pulsed Detonation Engine Thrust Production," AIAA 2002-4072, 38th AIAA/ASME/SAE/ASEE Joint Propulsion Conference, July 2002.

[2]Hoke, John, Bradley, Royce, Stutrud, Jeffrey, and Schauer, Fred, "Integration of a pulsed detonation engine with an ejector pump and with a turbo-charger as methods to self-aspirate," 40th AIAA Aerospace Sciences Meeting, AIAA 2002-0615, Jan 2002.

[3]Rouser, Kurt, King, Paul, Schauer, Fred, Sondergaard, Rolf, and Hoke, John, "Unsteady Performance of a Turbine Driven by a Pulse Detonation Engine." AIAA 2010-1116, 48th AIAA Aerospace Sciences Meeting, Jan 2010.

[4]Suresh, A., Hofer, D. C., Tangirala, V. E., "Turbine Efficiency for Unsteady, Periodic Flows." AIAA 2009-0504, 47th AIAA Aerospace Sciences Meeting, Jan 2009.

[5]Glaser, Aaron, Caldwell, Nicholas, Gutmark, Ephraim, "Performance of an Axial Flow Turbine Driven by Multiple Pulse Detonation Combustors." AIAA 2007-1244, 45th AIAA Aerospace Sciences Meeting, Jan 2007.

[6]Caldwell, Nicholas, Gutmark, Ephraim, "Performance Analysis of a Hybrid Pulse Detonation Combustor / Gas Turbine System." AIAA 2008-4880, 44th AIAA/ASME/SAE/ASEE Joint Propulsion Conference, July 2008.

[7]Vilimpoc, V., Goss, L., Sarka, B., "Spatial Temperature-Profile Measurements by the Thin Filament Pyrometry Technique," Optics Letters, Vol. 13, pp. 93-95, 1988.

[8]Meier GEA, "New Optical Tools for Fluid Mechanics", In Proc. 8th Int. Symp Flow Visualization, Sorrento, Italy, 1-4 September, 1998.

[9]Richard H, Rein M., Kompenhans J., and Meier GEA, "Demonstration of the Applicability of a Background Oriented Schlieren (BOS) Method". In Adrian (ed) Proc 10th Int Symp Appl Laser Techniques to Fkuid Mechanics, Lisbon, Portugal, 10-13 July 2000.

[10]Raffel M, Richard H., and Meier GEA, "On the Applicability of Background Oriented Optical Tomography for Large Scale Aerodynamic Investigations", Exp/ Fluids 28:477-481, 2000.

[11]Venkatakrishnan, L.and Meier GEA, "Density Measurements Using the Background Oriented Schlieren Techniques", Exp. Fluids 37:237-247, 2004.

[12]Blunck D., Kiel B., Goss L., and Lynch A.,"Spatial Development and Temperature of Spark Kernels Exiting into Quiescent Air", Submitted to the AIAA Journal, 2010.

[13]Developed at Innovative Scientific Solutions, Inc.